International Journal of Terrestrial Heat Flow and Applied Geothermics
VOL. 2, NO. 1 (2019); P. 30-36.
ISSN: 2595-4180
DOI: https://doi.org/10.31214/ijthfa.v2i1.27

IJTHFA
http://ijthfa.com/

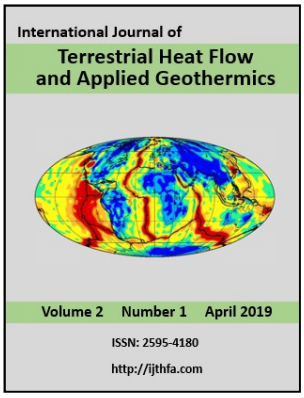

Keywords
Geothermal Field,
State of Tocantins,
Central Brazil.

Received: November 29, 2018

Accepted: February 27, 2019

Published: March 21, 2019

Regions of anomalous geothermal fields in the State of Tocantins, Central Brazil

Patricia Descovi [1], Fábio Vieira [1]

[1] Department of Geophysics, National Observatory, Rio de Janeiro, Brazil.

Email address
fabiovieira@on.br (F. Vieira)
Corresponding authors

Abstract
We report recent progress in determination of geothermal gradients and heat flow in the State of Tocantins, Central Brazil. This region lying between the Amazonas and Sao Francisco cratons has been affected by metamorphic folding events (Brasilia and Araguaia) during Proterozoic times. This area is also characterized by moderate micro-seismic seismic activity. Results of recent investigations have revealed the presence of several areas where geothermal gradients and heat flow have values higher than normal, which is considered atypical of stable tectonic settings. In southern parts of the State of Tocantins heat flow values are higher than 80 mW/m^2. Extrapolations based on near surface heat flow data point to crustal temperatures in excess of 200°C at depths less than 5 km. However, there are no evidences of magmatic intrusions at shallow intra-crustal depths. In the absence of other geologic source mechanisms and tectonic events the process responsible for high heat flow has been postulated to be enhanced heat transport by carbonic gas flow in the upper crust. This possible alternative is supported by observations of carbonic gas flow at sites of thermal springs within the study area and also in geothermal areas in the neighboring state of Goiás. Model simulations of deep crustal geotherms indicate that temperatures may approach levels of partial fusion at the crust mantle boundary.

1. Introduction

The State of Tocantins is situated in Central Brazil, in the region bounded by the structural provinces of Parnaiba, Tocantins and Sao Francisco (Almeida et al., 1977). These provinces are of Neoproterozoic age and arose from the collision of the Amazonas and Sao Francisco cratons (Heilbron et al., 2017). However, there are indications of recent tectonic activity, with emplacement of basic alkaline magmatic rocks of Neo-Cretaceous and Eocene ages (Almeida, 1986; Brod et al., 2005).

Recent studies led to identification of geophysical features associated with the alkaline intrusions (Marangoni et al., 2015; Azevedo, 2017; Hu et al., 2018; Tozer et al., 2017; Assumpção et al., 2017) also pointed out possible carbonic fluid flow in the upper crustal layers (Coelho e Moura, 2006; Padilha et al., 2013; Abdallah, 2016). Flow of fluids with dissolved carbon dioxide is considered responsible for occurrences of graphite veins in highly fractured terrains in the northern parts of Goiás and in the both the northern and southern parts of Tocantins (Giuliani et al., 1993; Luque et al., 1998; Arora et al., 1999; Solon et al., 2018). The origin of carbonic fluids is uncertain, but the possibility that pyrolysis of thermo-controlled sediments saturated with hydrocarbons was suggested. According to Sulem and Famin (2009), release of CO_2 from carbonate rocks by thermal decomposition led to weakening of fault zones and is consequently responsible of seismic activity. Such conditions are also believed to favor the widespread occurrence of thermal springs. Results of recent geothermal studies (Vieira e Hamza, 2012; Vieira et al., 2014; Vieira, 2015) confirmed the potential for occurrence of geothermal resources in the area.

Another notable feature is the presence of moderate seismic activity (Berrocal et al., 1984; Fernandes et al., 1991; Assumpção e Sacek., 2013; Assumpção et al., 2004; 2017). In spite of the presence of such neotectonic activity very few attempts have been made to determine geothermal characteristics of this region. In the present work, we report progress obtained in the evaluation of crustal temperature gradients and heat flow in the State of Tocantins, in Central Brazil.

2. Geological and Geophysical Settings

The connections between cratonic units in the study area were established along tectonic suture zones, known as Brasilia and Araguaia fold belts, which form a network of interfering orogens in the northern and western parts. The main tectonic units include the Rio dos Mangues, the Almas-

Cavalcante and the Goiano domains. The latter is dominant in the southern and southwestern parts (Hasui et al., 2012). The eastern parts are covered by phanerozoic sediments overlying the cratonic basement rocks (Góes, 1995). The locations of these units are shown in the simplified geologic map of Figure 1.

The main geologic features of the orogens were stitched together during the West Gondwana assembly about 630-520 Ma ago (Brito Neves et al., 2014; Frasca, 2015; Schmitt et al., 2018). The regional tectonics is marked by Quaternary fault systems, namely Estrondo (BR12) and Porangatu (BR19), as proposed for (Saadi et al, 2002), and lineaments (Araguaia-. Tocantins and Transbrazilian). The BR12 Fault is part of Araguaia-Tocantins Lineament

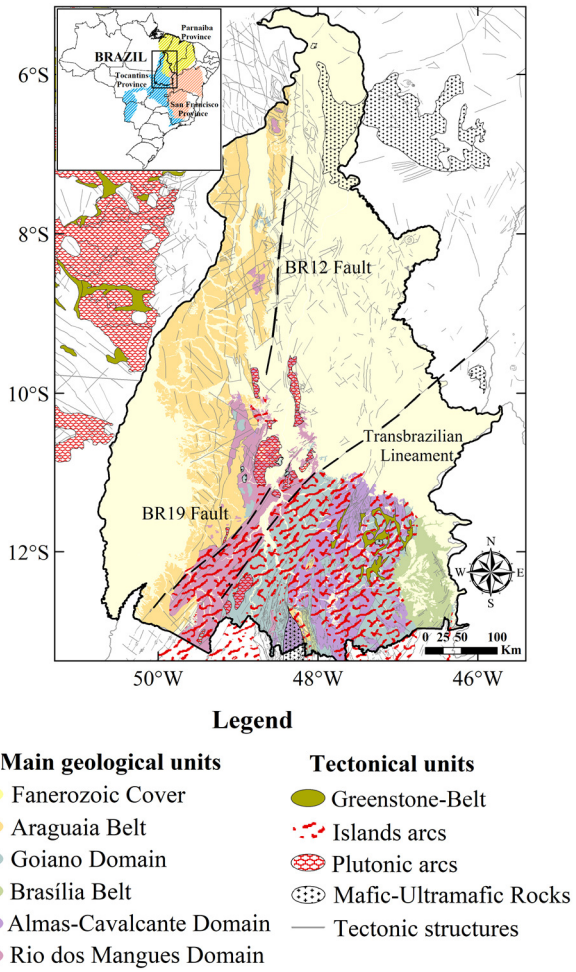

Figure 1 - Simplified geologic map of the study area and locations of the main structural features. The inset map in the top left corner indicates location of study area within the Brazilian territory.

3. Materials and Methods

Geothermal data acquired at 140 sites of the State of Tocantins and neighboring areas were analyzed in the present work. Manual measuring devices were used for field during the decades prior to 1990. Since 2000, digital data acquisition systems were employed for field measurements. During the early stages much of the subsurface temperature were measured using thermistor sensors calibrated against standard Platinum resistance thermometers. The locations of wells where temperature measurements were carried out are indicated in Figure 2.

Several different methods were used for determining temperature gradients, depending on the nature of techniques employed in acquisition of primary field data. These may be classified as incremental temperature logs (ITL), stable bottom temperature (SBT), bottom-hole temperature (BHT) and geochemical (GCL) methods. Hamza and Muñoz (1996), Gomes and Hamza (2005) and Vieira and Hamza (2012) have provided detailed descriptions of theory and use of these methods.

In the present work, ITL method was employed in determination of gradients (Γ) in fourteen wells, which presented near linear distributions of temperatures. Its calculation is determined by the linear adjustment of the temperature measurements (Ti) at discrete depth intervals (Zi) when the disturbance does not occur or is negligible.

In cases of non-linear distributions of temperatures, with indications of perturbations induced by groundwater flows, the deepest temperature was considered as the least perturbed. This method designated as SBT (stable bottom temperature) was used in evaluating gradient values in twenty-three wells.

The bottom-hole temperature method (BHT) was employed for data acquired in 9 deep wells drilled for oil exploration by PETROBRAS. The temperature data employed in BHT method has been corrected using a procedure similar to that suggested by the AAPG (1976).

In addition, geochemical data acquired by Geological Survey of Brazil (CPRM/SBG, 2006) in ninety-four groundwater wells were employed for determining reservoir temperatures based on silica geothermometry techniques (Fournier and Truesdell, 1973; Fournier, 1989; Swanberg e Morgan, 1978 and 1980). Recently, the methodology used in reservoir temperature estimates from concentrations of dissolved silica (SiO_2) was reassessed by Alexandrino and Hamza (2018).

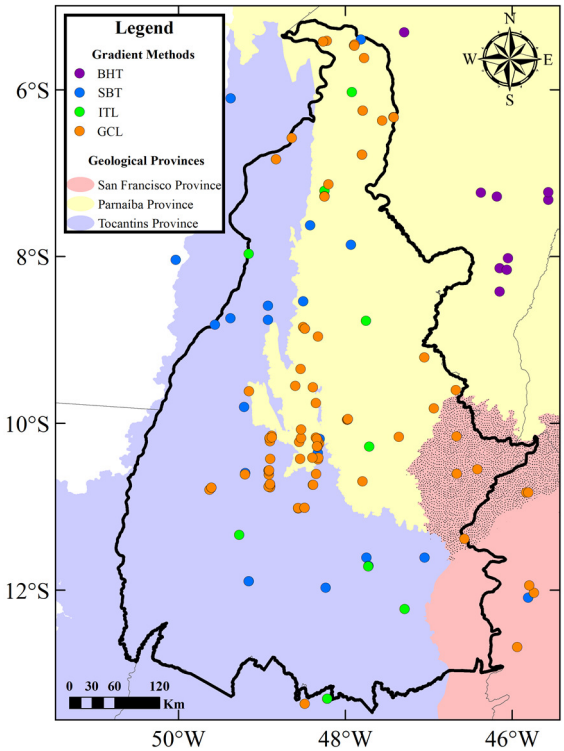

Figure 2 - Locations of geothermal in the State of Tocantins and neighboring areas. The background colors indicate the geological provinces.

Examples of temperature log data and procedures employed in determination of temperature gradients are illustrated in Figure 3 for wells in Santa Maria and Cristalandia. In Santa Maria well, temperatures recorded at depths greater than 120m have been employed for determining geothermal gradients. It has been linearly extrapolated to shallower depths corresponding to the values of mean annual surface temperature, as derived from local meteorological records, provided by the National Institute of Meteorology (INMET). The data for Cristalandia well was interpreted on the basis of the SBT method. Non-linear distributions of temperatures were observed in some boreholes, which were interpreted as arising from perturbations induced by groundwater flows.

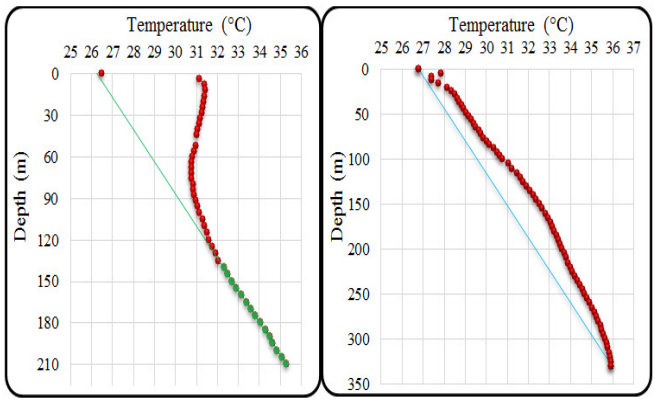

Figure 3 - Vertical distribution of temperatures in wells Santa Maria (left panel) and Cristalandia (right panel). Dots indicate log data. In the left panel the line indicates least square fit in ITL method for data in the interval 140 to 210 m; the line in the right panel refer to distribution of temperatures as per the SBT method.

Figure 4 illustrates examples of the use of BHT data acquired in oil wells (left panel) and the geochemical method (GCL) based on the silica content in groundwater wells (right panel). Details of the GCL method has been discussed in detail by Swanberg and Morgan (1978) and more recently by Alexandrino and Hamza, 2018).

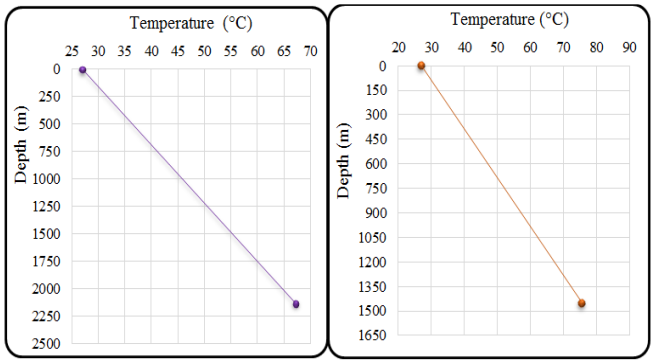

Figure 4 - Vertical distribution of temperatures in the wells Imperatriz (left panel) and Paraíso (right panel), by BHT (left panel) and GCL (right panel) methods, respectively (see text).

Thermal conductivity data refer to results of measurements carried out on core samples from six wells, values derived from geophysical well log data acquired in ten wells as well as estimated values based on chemical analysis of representative outcrops. During the decades of 1980 and 1990 measurements were carried out using the divided bar and line source apparatus. This changed with the acquisition of a commercially available plane source device. Calibrations of measurements were carried out using standard discs of fused silica and crystalline quartz and sub-standards of suitably selected rock samples. In the case of layered media, thermal conductivity values were calculated as weighted mean of the product of thicknesses and thermal conductivities of the main lithologic units. An example of this procedure is illustrated in Figure 5.

Heat flow values were calculated as the product of geothermal gradient (Γ) and mean thermal conductivity (λ) of the rock types in the selected interval. The values of mean and standard deviation (σ) of heat flow (q) was estimated using the relations:

$$q = \Gamma\,\lambda \pm (\sigma_\Gamma \lambda + \sigma_\lambda \Gamma) \qquad (1)$$

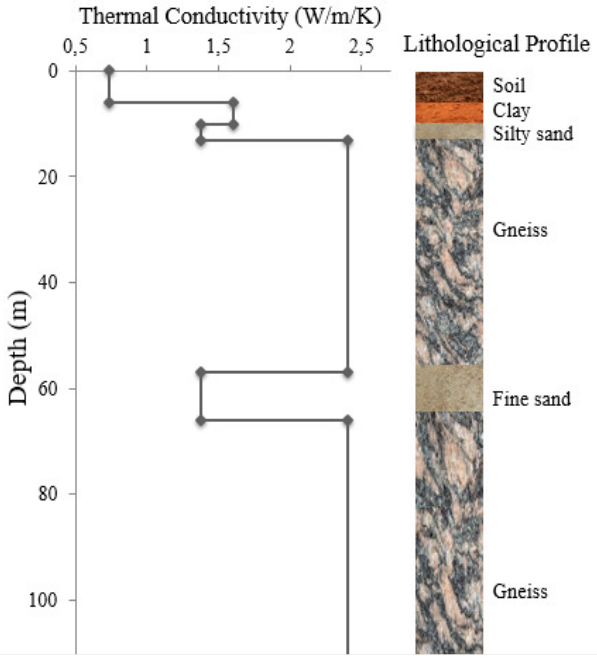

Figure 5 - Example of procedure used for thermal conductivity determination of layered media. Weighted mean was calculated based on the product of thicknesses and thermal conductivities of the main lithologic units.

4. Results

We present in the following details of the results obtained for geothermal gradients, thermal conductivity and heat flow in the study area.

4.1. Summary of Geothermal Gradients

Mean values geothermal gradients obtained with the different methods for the areal segments of the geologic units are provided in Table 1.

Values, falling in the range of 30 to 60°C/km were found in the south central and north central parts of the Tocantins province. The main outcrops in these areas belong to the Almas – Cavalcante, Goiano and Rio dos Mangues domains, notable for the presence of island arc features. In the remaining areas where the dominant outcrops are the Araguaia fold belt and sedimentary sequences of phanerozoic age. Lowest values of gradients of less than 20°C/km were encountered in the Jalapão area (at San Francisco Province), located in the northeastern parts, adjacent to the Sao Francisco craton.

Table 1 - Summary of geothermal gradient (Γ) values in the study area.

Geologic Unit	Methods	N	Γ (°C/km)	
			Range	Mean
Phanerozoic Cover	BHT, GCL	52	15-19	17.7
Araguaia Fold Belt	GCL, SBT, ITL	19	17-21	19.6
Sao Francisco Craton	GCL	7	13-17	15.7
San Francisco Basin	SBT, GCL	4	10-12	12.1
Almas Cavalcante Goiano Domain	SBT, ITL	11	27-31	29.6
Rio dos Mangues Domain	ITL, SBT, GCL	47	16-20	18.8

4.2. Thermal Conductivity

Thermal conductivity values of the main rock types within the geologic units are provided in Table 2. Sandstones were found to have values ranging from 2.8 to 4.7 W/m/K. This is also true of the sedimentary sequences encountered in the Jalapão area, located in the northeastern parts adjacent to the Sao Francisco craton. Lowest values were encountered for near surface samples of soil, clay, sand and silt. Samples of schists from the Almas – Cavalcante and Rio dos Mangues domains were found to have values in the range of 2.7 to 3.9 W/m/K

4.3. Heat Flow

Mean values of heat flow obtained by the different methods for the areal segments of the geologic units are listed in Table 3. Values, falling in this range 90 to 120 mW/m2 were found in the south central and north central parts of the Tocantins province. The main outcrops in these areas belong to the Almas – Cavalcante, Goiano and Rio dos Mangues geologic domains, notable for the presence of extinct island arc features.

Heat flow values fall in the range 70 to 100 mW/m^2, in areas of outcrops of Almas Cavalcante and Goiano Domain. Heat flow is in excess of 45 mW/m^2 areas of the Araguaia fold belt and in sedimentary sequences of Phanerozoic age. Low values of heat flow (< 45 mW/m^2) were encountered in the Jalapao area, located in the northeastern parts adjacent to the Sao Francisco craton.

5. Distributions of geothermal gradients and heat flow

Figure 6 illustrate the regional distribution of temperature gradients. Also shown in this figure are the outlines of local geologic provinces, basins and cratonic units (see legend in the inset on the top left corner). Note that gradients are >30ºC/km in the southern and north-central parts of the study area. These two high gradient regions appear to be separated by an east-west trending belt.

Table 2 - Thermal conductivity values of the main lithologic units in the study area.

Lithotype	Thermal Conductivity (W/m/K)	Reference
Sandstone	3.1 (Parnaíba Basin) 2.8 (SF Craton)	Pereira & Hamza (1991)
Fine grained sandstone	4.1	Pereira & Hamza (1991)
Medium grained sandstone	4.7	Pereira & Hamza (1991)
Shale	1.9	Pereira & Hamza (1991)
Silt	2.6	Pereira & Hamza (1991)
Argillite	1.8 (Parnaíba Basin) 2.7 (SF Craton)	Pereira & Hamza (1991)
Limestone	2.7	Pereira & Hamza (1991)
Mica schist	2.7	Pereira & Hamza (1991)
Quartzite	4.0	Vitorello et al (1980)
Schist	3.9	Vitorello et al (1980)
Phyllite	3.8 (Parnaíba Basin) 2.8 (SF Craton)	Vitorello et al (1980)
Meta-basalt	3.2	Vitorello et al (1980)
Gneiss	2.4	Vitorello et al (1980)
Granite	2.3	Vitorello et al (1980)
Marble	3.2	Vitorello et al (1980)
Granodiorite	3.1	Vitorello et al (1980)
Soil	0.7	Schön (2011), Yang & Wei (2017)
Clay	1.6	Schön (2011), Yang & Wei (2017)
Sand	1.4	Schön (2011), Yang & Wei (2017)
Silt	1.1	Schön (2011), Yang & Wei (2017)

Table 3 - Summary of heat flow values in the study area.

Geologic Unit	Methods	N	Heat Flow (mW/m^2)	
			Range	Mean
Almas Cavalcante and Goiano Domain	SBT, ITL	11	85-89	87,2
Araguaia Fold Belt	GCL, SBT, ITL	19	51-55	53,8
Phanerozoic Cover	BHT, GCL	52	47-51	49,8
Sao Francisco Craton	GCL	7	40-44	42,6
Rio dos Mangues Domain	ITL, SBT, GCL	47	40-44	42,1
San Francisco Basin	SBT, GCL	4	25-29	27,5

Figure 7 illustrates the regional distribution of heat flow in the study area. Heat flow is higher than 70mW/m^2 in the southern and northcentral parts. These two high heat flow regions appear to be separated by an east-west trending belt. This pattern is similar to that observed for geothermal gradients illustrated in Figure 6.

Also illustrated in this figure are the locations of epicenters of seismic activity, reported in studies of Assumpção et al (2004). These are indicated by black circles, the diameters of which are proportional to the magnitudes of seismic events, as

indicated in the inset on the top left corner. It is interesting to note the correspondence between the areas of high heat flow and seismic activity (monitored for the period of 1970 to 2018)

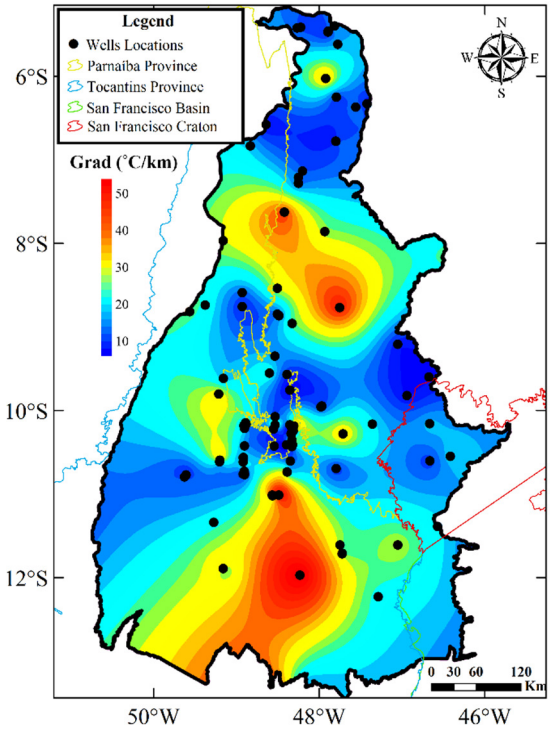

Figure 6 – Regional distribution of geothermal gradients. Thin curves indicate outlines of the main geologic provinces (see inset).

6. Crustal Geotherms

One dimensional thermal calculation was carried out under a purely conductive, steady state thermal regime. Following the standard practice, the parameter values were assumed constant, except for the radioactive heat generation which was assumed to decrease exponentially with depth in the upper crust. Such models have been discussed extensively in the literature (Carslaw and Jaeger, 1959; Singh e Jain, 1970; Hamza, 1982; Wang et al., 1996). In the case of a medium with thermal conductivity (λ) and internal heat generation by radioactive decay at the surface (A_o) the temperature T function of depth (z) may be expressed as:

$$T(z) = T_0 = \frac{A_0 D^2}{\lambda}\left(1 - exp\left(-\frac{z}{D}\right)\right) + \frac{(-A_0 D + q_0)}{\lambda} z \quad (3)$$

where T_0 is the temperature at depth z=0, and D is the logarithmic decrement of heat production with depth (Lachenbruch, 1970).

Parameter values adopted in the model calculations of the present work are given in Table 4. The value of D was assumed to be 11 km in the upper crust (Alexandrino, 2008). The values heat production Ao were calculated with from the abundances of radioactive elements Uranium (U), Thorium (Th) and Potassium (K), making use of the relation (Hamza and Beck, 1972; Rybach, 1976):

$$A_o = 10^{-5}\rho[9{,}52(U_{ppm}) + 2{,}56(Th_{ppm}) + 3{,}48(K_{\%})] \quad (2)$$

Figure 8 shows the calculated geotherms as well as partial meting curves for basalts in the lower crust and peridotites in the upper mantle. Three different melting curves were considered: dry or volatile free peridotite (Hirschmann, 2000), Peridotite with significant amounts CO_2 (Gudfinnsson & Presnall, 2005); and hydrated Peridotite (Wyllie, 1978). Note that temperature curves intersect the fusion curves in the lower crustal levels, in regions where heat flow is in excess of 80 mW/m^2. Thus, one may expect zones of partial melting in the lower crust in the southern parts of the Tocantins province.

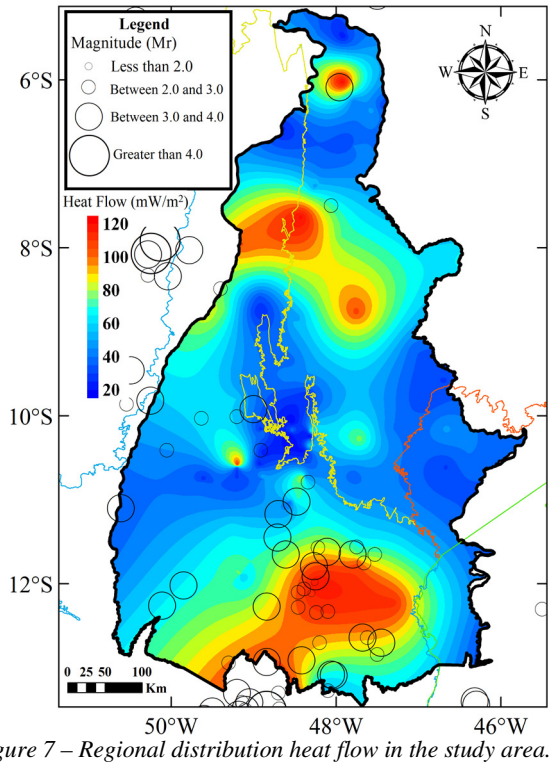

Figure 7 – Regional distribution heat flow in the study area. Thin curves indicate outlines of the main geologic provinces. The circles indicate locations micro seismic events (see legend in the inset).

Table 4 - Values of parameters used in model calculations.

Crustal Layer	Thickness (km)	Heat Production (μW/m^3)	Reference
Surface	<0.01	2.1 (Arquean Blocks)	Alexandrino, 2008 Vieira (2011)
		2.3 (Phanerozoic Blocks)	

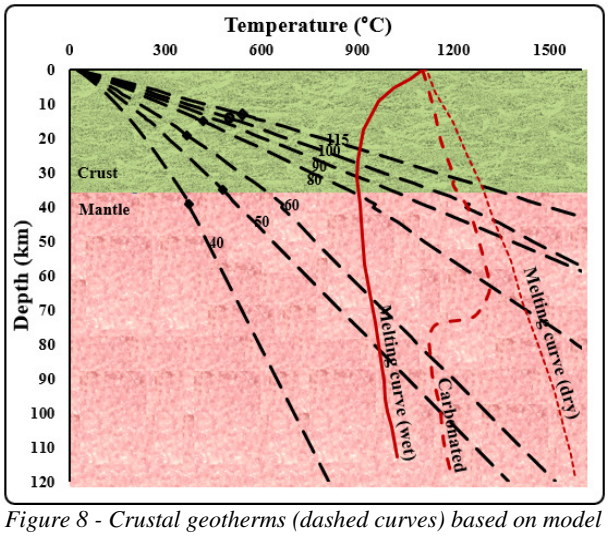

Figure 8 - Crustal geotherms (dashed curves) based on model simulations for the State of Tocantins. The numbers on the curves refer to heat flow values in mW/m^2.

7. Conclusions

Results of recent investigations have revealed the presence of several areas in the State of Tocantins where geothermal gradients and heat flow have values higher than normal, which is atypical of stable tectonic settings. In southern parts heat flow values are higher than 80 mW/m^2. Extrapolations based on near surface heat flow data point to crustal temperatures in excess of 200°C at depths of about 5 km. However, there are no evidences of magmatic intrusions at shallow intra-crustal levels. In the absence of other geothermal source mechanisms and tectonic events the process responsible for high heat flow has been postulated to be enhanced heat transport by carbonic gas flow in the upper crust. This possible alternative is supported by observations of carbonic gas flow at sites of thermal springs within the study area. Presence of gas flow has also been observed in geothermal areas in the neighboring state of Goiás. Model simulations of deep crustal geotherms suggest the possibility that temperatures approach levels of partial fusion at the crust mantle boundary.

8. Acknowledgments

The first author of this work is recipient of a post-graduate scholarship granted by CAPES. We thank the Department of Geophysics of the National Observatory for institutional support.

References

American Association of Petroleum Geologists – AAPG. 1976. Basic data file from AAPG Geothermal Survey of North America: Univ. of Oklahoma, Norman.

Abdallah, S. 2016. Geologia e Geoquímica do Grupo Riachão do Ouro na Folha Arraias: Evidências de Arco Magnético Paleoproterozóico. Geochimica Brasiliensis, 29(2).

Alexandrino, C.H., Hamza, V.M. (2018) Terrestrial Heat Flow in Non-Thermal Ground Water Circulation Settings of Brazil. International Journal of Terrestrial Heat Flow and Applications, 1(1), 46-51.

Almeida, F.F.M., Hasui, Y., Brito Neves, B.B., Fuck R.A. 1977. Províncias Estruturais Brasileiras. VIII Simpósio de Geologia do Nordeste, Campina Grande, Atas. Pernambuco, SBG - Núcleo Nordeste, 1, 363-392.

Almeida, F.F. 1986. Distribuição regional e relações tectônicas do magmatismo pós-paleozóico no Brasil. Revista Brasileira de Geociências, 16(4), 325-349.

Arora, B.R., Padilha, A.L., Vitorello, I., Trivedi, N.B., Fontes, S.L., Rigoti, A., Chamalaun, F.H. 1999. 2-D geoelectrical model for the Parnaíba Basin conductivity anomaly of northeast Brazil and tectonic implications. Tectonophysics, 302(1-2), 57-69.

Assumpção, M., Schimmel, M., Escalante, C., Rocha, M., Barbosa, J.R., Barros, L.V. 2004. Intraplate seismicity in SE Brazil: stress concentration in lithospheric thin spots, Geophysical Journal International, 159,390–399.

Assumpção, M., Sacek, V. (2013) Intra-plate seismicity and flexural stresses in Central Brazil. Geophys. Res. Lett., 40, 487-491, doi:10.1002/grl.50142.

Assumpção, M., Azevedo, P. A., Rocha, M. P., Bianchi, M.B. 2017. Lithospheric Features of the São Francisco Craton, in: Heilbron, M., Cordani, U. G., Alkmim, F.F. (Eds.), São Francisco Craton, Eastern Brazil: Tectonic Genealogy of a Miniature Continent. Springer International Publishing, Cham, p. 15–25.

Azevedo, P.A.D. 2017. Estudo do manto superior sob o Brasil utilizando tomografia sísmica de tempo de percurso com ondas P. Tese de Doutorado. Universidade de Brasília.

Berrocal, J., Assumpção, M., Antazena, R., Dias Neto, C. M., Ortega, R., França, H., Veloso, J.A.V. 1984. Sismicidade do Brasil, IAG/USP-CNEM, p. 320, São Paulo, Brazil.

Brito Neves, B.B.D, Fuck, R.A., Pimentel, M.M. 2014. A colagem brasileira na América do Sul: uma revisão. Revista Brasileira de Geologia, 44(3), 493-518.

Brod, J.A., Barbosa E.S.R., Junqueira-Brod T.C., Gaspar J.C., Diniz-Pinto H.S., Sgarbi P.B.A., Petrinovic L.A. 2005. The Late-Cretaceous Goiás Alkaline Province (GAP), Central Brazil. In: Comin-Chiaramonti P., Gomes C.B. (eds.), Mesozoic to Cenozoic alkaline magmatism in the Brazilian Platform. São Paulo, Edusp/Fapesp, p. 261-340.

Carslaw, H. S., Jaeger, J. C. 1959. Conduction of heat in solids: Oxford Science Publications. Oxford, England, p. 510.

Coelho, C. V., Moura, M. A. 2006. Mineralizações de Sn do Maciço Granítico Serra Branca, Goiás: evolução do sistema hidrotermal e fonte dos fluidos. Revista Brasileira de Geociências, 36(3), 513-522.

CPRM – Serviço Geológico do Brasil. 2006. Mapa de Geodiversidade do Brasil. Scale 1:1.000.000. Brasília.

Fernandes, E.P.; Blum, M.L.B., Ribeiro, R.K. 1991. The Goiás Seismic Zone - A new approach, paper presented at International Congress of the Brazilian Geophysical Society, Salvador, Brazil.

Fournier, R. O., & Truesdell, A. H. 1973. An empirical Na-K-Ca geothermometer for natural waters. Geochimica et Cosmochimica Acta, 37(5), 1255-1275.

Fournier, R. O. 1989. The solubility of silica in hydrothermal solutions: practical applications. Lectures on geochemical interpretation of hydrothermal water. UNU Geothermal Training Programme, Report, 10.

Frasca, A.A.S. 2015. Amálgamas do W-Gondwana na província Tocantins. Tese de Doutorado. Universidade de Brasília.

Giuliani, G., Olivo, G.R., Marini, O.J., Michel, D. 1993. The Santa Rita gold deposit in the Proterozoic Paranoá Group, Goiás, Brazil: an example of fluid mixing during ore deposition. Ore Geology Reviews, 8(6), 503-523.

Góes, A.M. 1995. Formação Poti (Carbonífero inferior) da Bacia do Parnaíba. Tese de Doutorado. Universidade de São Paulo.

Gomes, A.J., Hamza, V.M. 2005. Gradiente e Fluxo Geotérmico do Estado de Santa Catarina. In 9th International Congress of the Brazilian Geophysical Society & EXPOGEF, Salvador, Bahia, Brazil, 11-14 September 2005, p. 978-983. Society of Exploration Geophysicists and Brazilian Geophysical Society.

Gudfinnsson, G.H., Presnall, D.C. 2005. Continuous gradations among primary carbonatitic, kimberlitic, melilititic basaltic, picritic, and komatiiticmelts in

equilibrium with garnet lherzolite at 3-8 Gpa. Jour. Petrology, 46, 1645–1659.

Hamza, V. E., & Beck, A. E. 1972. Terrestrial heat flow, the neutrino problem, and a possible energy source in the Core. Nature, 240(5380), 343.

Hamza, V.M. 1982. Thermal Structure of the South American Continental Lithosphere During and Proterozoic. Revista Brasileira de Geociências, p.149-159. São Paulo, Brasil.

Hamza, V.M., Muñoz, M. 1996. Heat Flow Map of South America, Geothermics, 25, 599-646.

Hasui, Y., Carneiro, C.D.R., de Almeida, F.F.M., Bartorelli, A. 2012. Geologia do Brasil, p. 900, Beca.

Heilbron, M., Cordani, U.G., Alkmim, F.F., Reis, H.L. 2017. Tectonic Genealogy of a Miniature Continent. In São Francisco Craton, Eastern Brazil, p. 321-331. Springer, Cham.

Hirschmann, M.M. 2000. Mantle solidus: experimental constraints and the effects of peridotite composition. Geochem. Geophys. Geosyst. doi: 2000GC000070.

Hu, J., Liu, L., Faccenda, M., Zhou, Q., Fischer, K. M., Marshak, S., Lundstrom, C. 2018. Modification of the Western Gondwana craton by plume–lithosphere interaction. Nature Geoscience, 11(3), 203.

Lachenbruch, A.H. 1970. Crustal temperature and heat production: Implications of the linear heat-flow relation. Journal of Geophysical Research, 75(17), 3291-3300.

Luque, F.J., Pasteris, J.D., Wopenka, B., Rodas, M., Barrenechea, J.F. 1998. Natural fluid-deposited graphite: mineralogical characteristics and mechanisms of formation American Journal of Science, 298, 471–498.

Marangoni, Y.R., Zhang, H., Ferreira, H.J. 2015. Gravity and magnetic integrated data interpretation of the Corrégo dos Bois complex, Goiás alkaline province, Central Brazil. Brazilian Geophysical Journal, 33(4), 599-610.

Padilha, A.L., Vitorello, I., Pádua, M.B. 2013. Deep conductivity structure beneath the northern Brasília belt, central Brazil: Evidence for a Neoproterozoic arc-continent collision. Gondwana Research, 23(2), 748-758.

Pereira, A.J.O., Hamza, V.M. 1991. Geothermal Heat Flux in the Parnaiba Basin (In Portuguese), Proceedings of the 2o International Congress of the Brazilian Geophysical Society, Salvador (BA), 1, 177-182.

Rybach, L. 1976. Radioactive heat production in rocks and its relation to other petrophysical parameters. Pure and Applied Geophysics, 114(2), 309-317.

Saadi, A., Dart, R. L., Machette, M.N. 2002. Map of quaternary faults and lineaments of Brazil. Project of international lithosphere program task group II-2, major active faults of the world, University of Minas Gerais and US Geological Survey.

Schmitt, R., de Araújo Fragoso, R., Collins, A. S. 2018. Suturing Gondwana in the Cambrian: The Orogenic Events of the Final Amalgamation. In Geology of Southwest Gondwana, p. 411-432. Springer, Cham.

Schön, J. 2011. Physical properties of rocks: A workbook, 8. Elsevier.

Singh, R.M., Jain S.C. 1970. On Temperatures in the Crust: Effect of temperature Dependence of Conductivity. Pure and Applied Geophysics, 80(1), 267-270.

Solon, F.F., Fontes, S.L., La Terra, E.F. 2018. Electrical conductivity structure across the Parnaíba Basin, NE Brazil. Geological Society, London, Special Publications, 472, SP472-19.

Sulem, J., Famin, V. 2009. Thermal decomposition of carbonates in fault zones: Slip-weakening and temperature-limiting effects. Journal of Geophysical Research: Solid Earth, 114 (B3).

Swanberg, C. A., Morgan, P. 1978. The linear relation between temperatures based on the silica content of groundwater and regional heat flow: a new heat flow map of the United States. Pure and Applied Geophysics, 117(1-2), 227-241.

Swanberg, C. A., Morgan, P. 1980. The silica heat flow interpretation technique: assumptions and applications. Journal of Geophysical Research: Solid Earth, 85(B12), 7206-7214.

Tozer, B., Watts, A.B., & Daly, M.C. 2017. Crustal structure, gravity anomalies, and subsidence history of the Parnaíba cratonic basin, Northeast Brazil. Journal of Geophysical Research: Solid Earth, 122(7), 5591-5621.

Vieira, F.P.; Hamza, V.M. 2012. Lateral flow of groundwater in sedimentary basins: Implications for Occurrence of Geothermal Resources (in Portuguese), Proceedings, V Brazilian Geophysical Symposium, Salvador (BA).

Vieira, F.P., Hamza, V.M., Alexandrino, C.H. 2014. Obliteration of thermal springs by groundwater flows in sedimentary basins of Brazil. Hydrogeology Journal, 22, x21, 2014.

Vieira, F.P. 2011. Representação Global do Fluxo de Calor Mantélico. Dissertação de Mestrado. Observatório Nacional.

Vieira, F.P. 2015. Energia Geotérmica de média e alta entalpia no Brasil: Avaliações de recursos e perspectivas de aproveitamento. Ph.D. Thesis. Observatório Nacional, Rio de Janeiro (Brazil).

Vitorello, I.; Hamza, V.M.; Pollack, H.N. 1980. Terrestrial Heat Flow in the Brazilian Highlands, Journal of Geophysics Review, 85, 3778- 3788.

Yang, S., Wei, J. 2017. Fundamentals of Petrophysics. Springer Berlin Heidelberg.

Wang, Ji Yang et al. 1996. Geothermics in China. Seismological Press Beijing, China, 10(2), ISBN 7-5028-1364-0/P 853.

Wyllie, P.J. 1978. Mantle fluid compositions buffered in peridotite–CO_2–H_2O by carbonates, amphibole, and phlogopite Jour Geol, 86, 687–713.